PCCP

Accepted Manuscript

This is an *Accepted Manuscript*, which has been through the Royal Society of Chemistry peer review process and has been accepted for publication.

Accepted Manuscripts are published online shortly after acceptance, before technical editing, formatting and proof reading. Using this free service, authors can make their results available to the community, in citable form, before we publish the edited article. We will replace this *Accepted Manuscript* with the edited and formatted *Advance Article* as soon as it is available.

You can find more information about *Accepted Manuscripts* in the Information for Authors.

Please note that technical editing may introduce minor changes to the text and/or graphics, which may alter content. The journal's standard Terms & Conditions and the Ethical guidelines still apply. In no event shall the Royal Society of Chemistry be held responsible for any errors or omissions in this *Accepted Manuscript* or any consequences arising from the use of any information it contains.

ROYAL SOCIETY OF CHEMISTRY

www.rsc.org/pccp

Cite this: DOI: 10.1039/c0xx00000x

www.rsc.org/xxxxxx

COMMUNICATION

Experimental validation of 'Pnicogen Bonding' in Nitrogen from charge density analysis

Sounak Sarkar, Mysore S. Pavan and T. N. Guru Row*

Received (in XXX, XXX) Xth XXXXXXXXX 20XX, Accepted Xth XXXXXXXXX 20XX
DOI: 10.1039/b000000x

The participation of nitrogen atom acting as an electrophile in pnicogen bonding, a hitherto unexplored interaction has been established using experimental charge density analysis. QTAIM and NBO analyses ratify this observation.

In past few decades there have been rigorous studies on non-covalent interactions and their role in chemical reactions, molecular recognition, and biochemical processes both in terms of theoretical and experimental approaches.[1] Among them hydrogen bonding has received the utmost attention due to its frequency of occurrence in chemical and biological systems. Its conformation guiding ability in biomolecules such as proteins, DNA and carbohydrates is well documented.[2] Halogen bonding, another non-covalent interaction, has shown its prominence in constructing supramolecular assemblies in soft and electronic materials, anion sensors, porous and inclusion (drug-receptor) complexes.[3] In recent times other non-canonical interactions, chalcogen bonding and tetrel (carbon) bonding has been subjected to extensive theoretical and spectroscopic evaluation.[4] All these interactions are of electrostatic origin and have been well construed in terms of Politzer's σ-hole concept on the donor atoms.[5] Experimental charge density analysis has proved to be the gold standard to unequivocally establish the existence of the σ-hole and has provided the platform for topological exploration of the bonding aspects.[6] The relevance of carbon bonding and chalcogen bonding has been addressed by experimental charge density analysis and the results allow for the quantification of the strength and directionality in such interactions.[7] Based on similar arguments, pnicogen bond is a Lewis acid−Lewis base interaction involving elements of group15 as an electron-pair acceptor. After the appearance of first paper on P•••P pnicogen interaction,[8] several theoretical investigations have been carried out to establish the relevance of pnicogen bonding in supramolecular architecture.[9] In addition, recent reports have addressed the capability of N atom to involve in pnicogen bonding based on theoretical estimates of interaction energies as well as CSD based analysis. However, it is noteworthy that no detailed experimental analysis is found in literature to establish the σ hole on nitrogen atom and consequently establish the presence of pnicogen bond.[10] In this communication, we have attempted to establish pnicogen bonding involving nitrogen atom using high resolution X-ray charge density analysis along with theoretical calculations (gas phase NBO and periodic DFT calculations). Further, the propensity of nitrogen atom to display anisotropic electron density distribution to assist the formation of pnicogen bond in crystal structures has been investigated.

Cambridge Structural Database (CSD) analysis has been carried out on crystal structures (version 5.35, Nov 2013) with the following geometric criteria: a) the distance between the nucleophile X and the nitrogen atom is within the sum of the van der Waal radii, b) the angle $\angle X_1$–N•••X is constrained to lie between 165°–180° to ensure the most probable σ-hole interaction at the nitrogen atom thus avoiding potential X•••H–N hydrogen bonds and reduced repulsive interaction between the nucleophile and nitrogen atom (Figure 1 (a)).[5b,11] Also because of this angular constraint (b) the maximal angular distribution(∠ N-H•••X (Figure 1(b)) lies in the range of 90°-115° which classifies the bifurcated N-H•••X H-bonding as weak and less probable.[12] (F-4 in ESI) This resulted in a total of 371 hits, 37 of these hits include biologically active molecules (see S-2, T-4,T-5 and F-3 in ESI). Based on a careful evaluation of the geometrical features derived from the CSD analysis, a co-crystal of 2-Amino-5-Nitropyridine and 2-chloroacetic acid was chosen for a detailed analysis (Figure 2; **(I)** N•••Cl=3.283Å and ∠C–N•••Cl=175.26°; N–H•••Cl=2.951Å, 2.962Å and ∠N–H•••Cl=104.57°, 104.49°).[13] The structure represents the possibility of having either (a) or (b) interaction motif shown in Figure 2 since the N•••Cl distance is at the threshold of the sum of the van der Waal radii (3.30 Å) and the formation of a weak N–H•••Cl hydrogen bond is indicated.

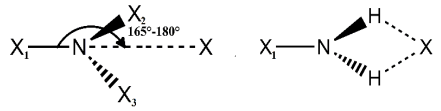

(a) **(b)**

Fig. 1 (a) Probable 'pnicogen bonding' geometry with X as acceptor atom (where X = O, N, S, Cl etc.) directing towards the nitrogen atom, and **(b)** the less probable bifurcated weak N–H•••X hydrogen bonded motif

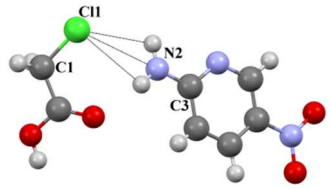

(**I**)

Fig. 2 Structural motif containing the plausible N•••Cl interaction in the co-crystal of 2-amino-5-nitropyridine and chloroacetic acid. (**I**)

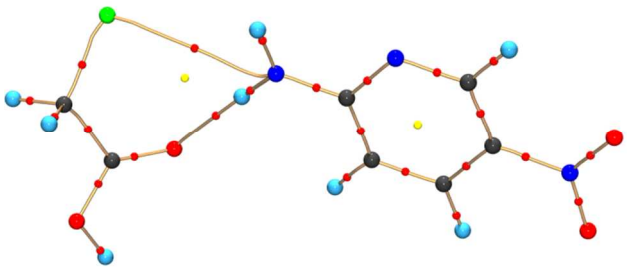

Fig. 3 Molecular Graph showing experimental bond paths along with bcps of the existing intermolecular interactions in the structural motif (**I**) The yellow dots represents the (3,+1) ring critical points(RCP) while the red dots represents the (3,-1) bond critical points (BCP).The curved segments signifies the bond paths between atoms.

However, it should be noted that the crystal structure of (**I**) is stabilized by typical N–H•••O, O–H•••N hydrogen bonding along with π–π stacks.

Experimental charge density along with the theory of 'Atoms in Molecules' (AIM) provides the most suited framework for the characterization of the 'pnicogen bond' in terms of bonding densities. A high resolution X-ray diffraction data (sinθ/λ=1.08 $Å^{-1}$) collected at 100K on a good quality crystal grown from methanol provides the experimental basis for using Hansen and Coppens multipole formalism.[14] The results from the experimental model have been compared with theoretical model generated through periodic DFT calculations using Crystal 09.

The presence of (3,–1) Bond Critical Point (bcp) between N(2) and Cl atoms (R_{ij} = 2.968Å) atom establishes the presence of the pnicogen bond. However the existence of commonly anticipated N-H•••Cl hydrogen bond can be ruled out based on clear absence of bcp between H atoms and Cl (Figure.3). The angle of ∠C3–N(2)•••Cl1 =174.98°(5) favours the formation of σ–hole at nitrogen atom in terms of the geometry. The topological features of the electron density corresponding to N•••Cl bond from both experimental and theoretical models (Table 1) ascertain the existence of pnicogen bonding unequivocally. The magnitude of the interaction energy calculated based on the EML method is at par with those of carbon bonding (C•••O = -5.9 $kJmol^{-1}$) and halogen bonding involving F, Cl (F•••F = -8.9 $kJmol^{-1}$, Cl•••Cl= -4.3±1.0 $kJmol^{-1}$) respectively.[7,15]

The 3D deformation map and 2D Laplacian map calculated from the experimental modelling confirm the presence of σ-hole on N(2) site (Figure 4a, b). It is observed that the valence shell charge concentration (VSCC) region of Cl atom faces the charge depleted site at the nitrogen atom (Figure 4a) while in Figure 4b, charge accumulation in the form of lumps in the VSCC of Cl atom faces the hole at nitrogen atom.

The experimental and theoretical 3D electrostatic potential (ESP) map plotted at 0.5 $eÅ^{-3}$ iso-density surface (Figure 5) reveals the electropositive region at the nitrogen atom, akin to the σ-hole features in halogen/chalcogen/carbon bonding.[7,15] The appearance of σ-hole along the C–N covalent bond and the moderately negative ESP on the Cl atom certifies a classical δ^{+}•••δ^{-} type of interaction. The positive site (δ^{+} on the amino N(2)) is formed due to the combined –I and –R effects from the nitro substituted pyridine ring. This is quite fascinating as it can be experimentally observed that nitrogen atom despite being highly electronegative and less polarisable in nature offers scope for pnicogen bonding.

Table 1 Topological values of N•••Cl interaction at bcp **I**

N···Cl	Rij(Å)	ρ($eÅ^{-3}$)	$\nabla^2\rho$($eÅ^{-5}$)	$\lvert V_{bcp}\rvert/G_{bcp}$	E_{int}($kJmol^{-1}$)
Experiment	2.9677	0.054(6)	0.790(2)	0.80	-7.1
Theory	2.9042	0.064(0)	0.872(0)	0.84	-8.7

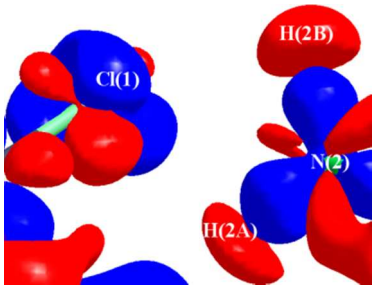

(a)

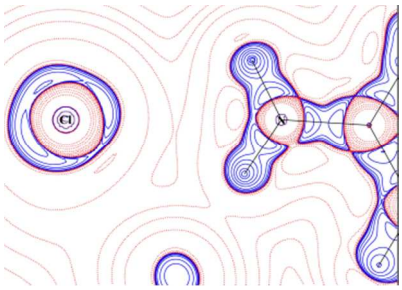

(b)

Fig. 4 (a) Experimental 3D deformation density map drawn on isosurface of ± 0.08$eÅ^{-3}$ (b) 2D plot of Laplacian map drawn at logarithmic scale. In both cases, +ve and –ve regions are depicted in blue and red respectively

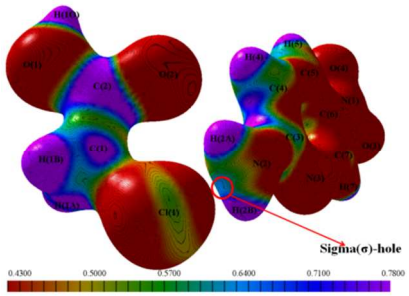

(a)

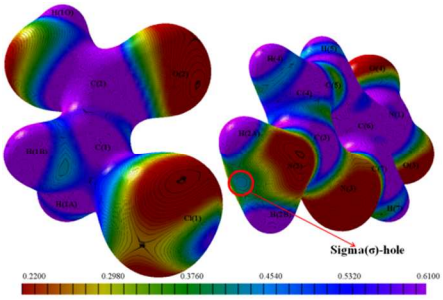

(b)

Fig. 5 ESP mapped on the isodensity surface drawn at 0.5$eÅ^{-3}$ **(a)** experiment; **(b)** theory, showing the possible σ-hole depicted in sky blue. The red part on colour bar indicates extreme electronegative region while the violet indicates relative extreme electropositive region

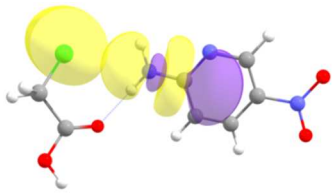

(a)

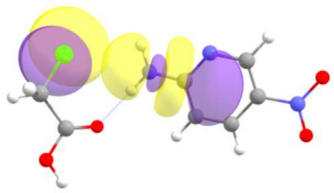

(b)

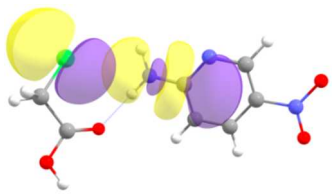

(c)

Fig. 6 NBO analysis portrayal of the two lone pair (lp) orbitals (a) , (b) and (c) of Cl atom involved in charge-transfer interaction with σ*C-N anti-bonding orbital respectively. The yellow colour depicts the positive lobes while violet colour indicates negative lobes.

The observations made by the topological analysis in the solid state were further corroborated by NBO analysis.[16] The co-ordinates for the analysis of Dimer (**I**) are derived from the results of the multipole model. The NBO analysis for the participating monomeric units, donor chloroacetic acid (Clacac) and acceptor 2-amino-5-nitropyridine (2-A5NP) have been carried out using the same set of coordinates. The results emphasizes interorbital interactions in terms of charge transfer from the three chlorine lone pair orbitals (represented as LP (1) Cl, LP (1) Cl and LP (3) Cl) of Clacac to the anti-bonding σ* N(2)–C(3) orbital (BD*(1) N–C) (Figure 6a,b,c**;** Table 2). Stabilisation energies (second-order perturbation energies E(2)) corresponding to the charge transfers are 0.67kJmol^{-1},1.05 kJmol^{-1} and 1.63kJmol^{-1} respectively (Table 2). Similar conclusions can be made on the account of orbital energy and orbital occupancy changes of the participating orbitals in N•••Cl pnicogen bonding interaction (see S-1 in ESI).

The NBO calculation also suggests that the amino N(2) is having a prolific sp^2 character which prompted us to examine the ellipticity profile for the N(2)–C(3) bond obtained from the topological analysis (Figure 7).[17] This indicates that there is a considerable charge transfer from N(2) atom to the pyridine ring substantiating the observed trigonal planar geometry of amino moiety in (**I**).

It is of interest to note that the CSD analysis described in the beginning also indicates that the probability of pnicogen bond formation is high in cases where nitrogen atom is in conjugation with a π electron system. Indeed, the propensity of pnicogen bond formation is most pronounced when the nitrogen moiety is planar (X_1-N-X_2-X_3; inset in Figure 8). This can be

Table 2. NBO analysis of monomer and dimer

	Type of NBO	Orbital Energy (au)	Orbital Occupancy
2-A5NP	BD*(1) N-C	0.5343	0.0222
Clacac	LP (1) Cl	-0.9645	1.9972
	LP (2) Cl	-0.4008	1.9760
	LP (3) Cl	-0.3984	1.9653
Dimer (**I**)	BD* (1) N-C	0.5598	0.0235
	LP (1) Cl	-0.9959	1.9971
	LP (2) Cl	-0.4315	1.9757
	LP(3) Cl	-0.4287	1.9653
Net change after charge transfer	BD* (1) N-C	0.0256	0.0013
	LP (1) Cl	-0.0314	-0.0001
	LP (2) Cl	-0.0307	-0.0004
	LP(3) Cl	-0.0303	-0.0007
Stabilisation Energy (kJ/mol)	LP (1)Cl→ BD*(1)N-C	0.6694	
	LP (2)Cl→ BD*(1)N-C	1.0460	
	LP (3)Cl→ BD*(1)N-C	1.6318	

understood from the VSEPR theory, i.e., when the lone pair of nitrogen is involved in resonance, the N-centric moiety undergoes a change in geometry from pyramidal to trigonal planar geometry The lone pair-bond pair (lp-bp) repulsion gets reduced compared to that in a pyramidal geometry thereby causing widening of the X_2-N-X_3 framework which ensures the approach of the nucleophile towards the σ-hole on nitrogen atom.[18]

In conclusion, the first experimental proof for the existence of σ-hole on the nitrogen atom, one of the most electronegative elements and the first congener of pnictide family, is demonstrated. The main aspect of the present study is to understand the prospect of σ-hole interactions involving nitrogen atom, especially when forced into a planar configuration to form a weak but highly directional interaction with a nucleophile resulting in a pnicogen bond.

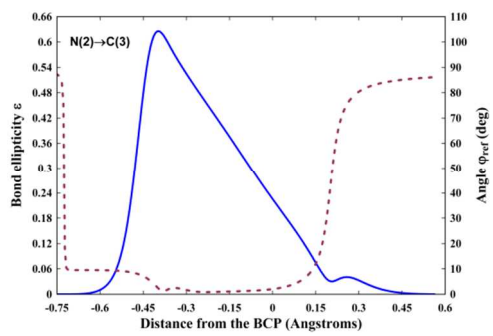

Fig. 7 Ellipticity profile of N(2)-C(3) bond in the pyridine ring. The blue curve represents the bond ellipticity (ε) values and the red dot curve represents the angle Φ_{ref},which is the angle between the eigenvector of the principal axis of ellipticityλ_2 and the π-plane of the pyridine ring.

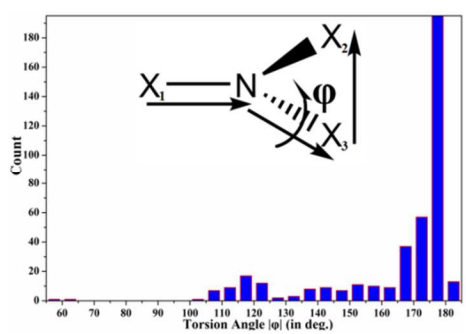

Fig. 8 Histogram of all structures with N•••X 'pnicogen bond'

Notes and references

Solid state and Structural Chemistry Unit, Indian Institute of Science Bangalore 560012, India. Fax: (+) 91-080-23601310 E-mail: ssctng@sscu.iisc.ernet.in

† Electronic Supplementary Information (ESI) available: [Data collection, refinement details, theoretical calculations, crystallographic data and diagrams. CCDC 1019123]. See DOI: 10.1039/b000000x/

Experimental Section

A high-resolution dataset of **I** was collected on a Oxford Xcalibur (Mova) diffractometer[18] equipped with an EOS CCD detector using *MoKα* radiation (λ= 0.71073 Å) and a Mova microscource. The single crystal was afixed to a Hampton Research Cryoloop using Paratone-N oil and was cooled with a liquid nitrogen stream using an Oxford Cryostream nitrogen gas-stream cooling device. Crystal data for **I**: $C_7H_8ClN_3O_4$ (M =233.61 g/mol): monoclinic, space group Cc (no. 9), a = 4.81980(10) Å, b = 21.7824(3) Å, c = 9.3616(2) Å, β = 104.264(2)°, V = 952.54(3) Å^3, Z = 4, $2\theta_{max}$=100.28, completeness=96.3%, ρ_{calc} = 1.629 g/cm^3, μ(MoKα) = 0.400 mm^{-1}, 52673 reflections measured, 9688 unique, R1(I>2σ(I))=0.025, wR2(I>2σ(I))=0.045, GoF=0.9060 after multipole refinement. The structure was solved by direct methods (SHELXS-97).[19] An IAM was refined with SHELXL-97. The multipole refinement with XD2006 [20] was carried out against F^2 with a sigma cutoff of 2 (see the Supporting Information) using 11 resolution dependent scale factors. Anisotropic displacement parameters for the hydrogen atoms were calculated with SHADE[21] using a riding model with neutron diffraction standard bond distances to the carbon atoms. XD2006 was used for the multipole refinement.

1 P. Hobza and R. Zahradník, *Weak intermolecular interactions in chemistry and biology*, 1978.
2 (a)S. Scheiner, *Hydrogen bonding. A theoretical perspective*, 1997; (b)G. A. Jeffrey, *An introduction to hydrogen bonding*, Oxford university press New York, 1997.
3 (a)P. Metrangolo, F. Meyer, T. Pilati, G. Resnati and G. Terraneo, *Angew. Chem. Int. Ed.*, 2008, **47**, 6114-6127; (b)P. Metrangolo and G. Resnati, eds., *Halogen bonding: fundamentals and applications*, Springer, 2008.
4 (a)C. Bleiholder, D. B. Werz, H. Köppel and R. Gleiter, *J. Am. Chem. Soc.*, 2006, **128**, 2666-2674; (b)D. Mani and E. Arunan, *Phys. Chem. Chem. Phys.*, 2013, **15**, 14377-14383; (c)S. A. Yao, K. M. Lancaster, A. W. Götz, S. DeBeer and J. F. Berry, *Chem. Eur. J.*, 2012, **18**, 9179-9183; (d)A. Bauzá, T. J. Mooibroek and A. Frontera, *Angew. Chem. Int. Ed.*, 2013, **52**, 12317-12321.
5 (a)J. S. Murray, P. Lane and P. Politzer, *Int. J. Quantum Chem*, 2007, **107**, 2286-2292; (b)P. Politzer, J. S. Murray and T. Clark, *Phys. Chem. Chem. Phys.*, 2013, **15**, 11178-11189; (c)P. Politzer and J. S. Murray, *ChemPhysChem*, 2013, **14**, 278-294; (d)P. Politzer, J. S. Murray and T. Clark, *Phys. Chem. Chem. Phys.*, 2010, **12**, 7748-7757; (e)A. Bundhun, P. Ramasami, J. S. Murray and P. Politzer, *J. Mol. Model.*, 2013, **19**, 2739-2746.
6 T. S. Koritsanszky and P. Coppens, *Chem. Rev.*, 2001, **101**, 1583-1628.
7 (a)S. P. Thomas, M. S. Pavan and T. N. Guru Row, *Chem. Commun.*, 2014, **50**, 49-51; (b)M. E. Brezgunova, J. Lieffrig, E. Aubert, S. Dahaoui, P. Fertey, S. Lebegue, J. G. Angyan, M. Fourmigue and E. Espinosa, *Cryst. Growth Des.*, 2013, **13**, 3283-3289.
8 S. Zahn, R. Frank, E. Hey-Hawkins and B. Kirchner, *Chem. Eur. J.*, 2011, **17**, 6034-6038.
9 S. Scheiner, *Acc. Chem. Res.*, 2012, **46**, 280-288.
10 (a)S. Scheiner, *J.Chem.Phys.*, 2011, **134**, 164313; (b)P. Politzer, J. S. Murray, G. V. Janjić and S. D. Zarić, *Crystals*, 2014, **4**, 12-31; (c)S. Scheiner, *Chem. Phys. Lett.*, 2011, **514**, 32-35; (d)I. Alkorta, G. Sánchez-Sanz, J. Elguero and J. E. Del Bene, *J.Phys.Chem. A*, 2012, **117**, 183-191.
11 B. Jeziorski, R. Moszynski and K. Szalewicz, *Chem. Rev.*, 1994, **94**, 1887-1930.
12 T. Steiner, *Angew. Chem. Int. Ed.*, 2002, **41**, 48-76.
13 Y. Le Fur, M. Bagieu-Beucher, R. Masse, J.-F. Nicoud and J.-P. Lévy, *Chem. Mater.*, 1996, **8**, 68-75.
14 (a)R. F. Bader, *Atoms in molecules*, Wiley Online Library, 1990; (b)N. K. Hansen and P. Coppens, *Acta Crystallographica Section A: Crystal Physics, Diffraction, Theoretical and General Crystallography*, 1978, **34**, 909-921.
15 (a)M. S. Pavan, K. D. Prasad and T. N. Guru Row, *Chem. Commun.*, 2013, **49**, 7558-7560; (b)M. E. Brezgunova, E. Aubert, S. Dahaoui, P. Fertey, S. b. Lebègue, C. Jelsch, J. n. G. Ángyán and E. Espinosa, *Cryst. Growth Des.*, 2012, **12**, 5373-5386; (c)E. Espinosa, E. Molins and C. Lecomte, *Chem. Phys. Lett.*, 1998, **285**, 170-173.
16 A. E. Reed, L. A. Curtiss and F. Weinhold, *Chem. Rev.*, 1988, **88**, 899-926.
17 (a)J. Cheeseman, M. Carroll and R. Bader, *Chem. Phys. Lett.*, 1988, **143**, 450-458; (b)R. Pal, S. Mukherjee, S. Chandrasekhar and T. N. Guru Row, *J. Phys. Chem. A*, 2014, **118**, 3479-3489.
18 *Agilent Technologies CrysAlis, PRO*, (2010).
19 G. M. Sheldrick, *Acta Crystallogr. Sect. A: Found. Crystallogr.*, 2007, **64**, 112-122.
20 T. Koritsanszky, P. Macchi, C. Gatti, L. Farrugia, P. Mallinson, A. Volkov and T. Richter, *A Computer Program Package for Multipole Refinement and Topological Analysis of Charge Densities and Evaluation of Intermolecular Energies from Experimental or Theoretical Structure Factors, Version*, 2007, **5**.
21 A. O. Madsen, *J. Appl. Crystallogr.*, 2006, **39**, 757-758.

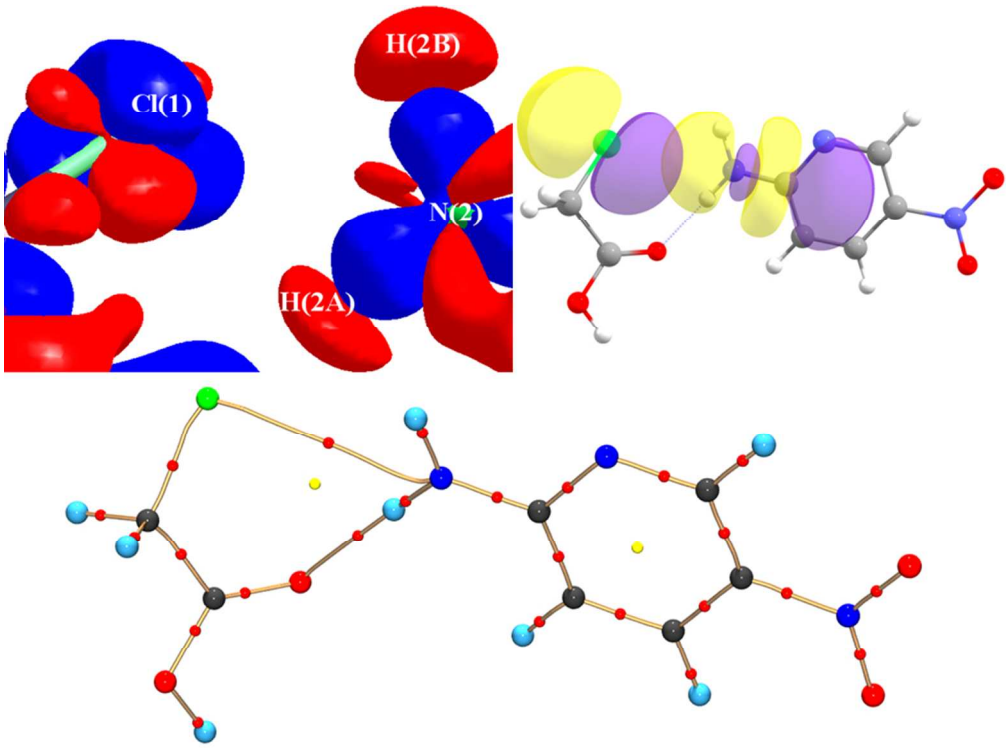

254x190mm (96 x 96 DPI)